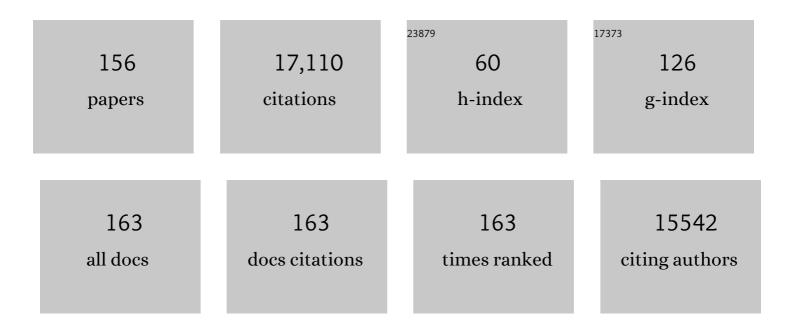
Pierre-Francois Van de Moortele

List of Publications by Year in descending order

Source: https://exaly.com/author-pdf/5717812/publications.pdf Version: 2024-02-01



#	Article	IF	CITATIONS
1	A nineâ€channel transmit/receive array for spine imaging at 10.5 T: Introduction to a nonuniform dielectric substrate antenna. Magnetic Resonance in Medicine, 2022, 87, 2074-2088.	1.9	9
2	Presurgical Functional Localization Possibilities, Limitations, and Validity. Medical Radiology, 2022, , 343-372.	0.0	1
3	Identifying symptomatic trigeminal nerves from MRI in a cohort of trigeminal neuralgia patients using radiomics. Neuroradiology, 2022, 64, 603-609.	1.1	5
4	Magnetic field strength dependent SNR gain at the center of a spherical phantom and up to 11. <scp>7T</scp> . Magnetic Resonance in Medicine, 2022, 88, 2131-2138.	1.9	21
5	Flow residence time in intracranial aneurysms evaluated by in vitro 4D flow MRI. Journal of Biomechanics, 2022, 141, 111211.	0.9	6
6	Progress in Imaging the Human Torso at the Ultrahigh Fields of 7 and 10.5ÂT. Magnetic Resonance Imaging Clinics of North America, 2021, 29, e1-e19.	0.6	10
7	A Diffeomorphic Vector Field Approach to Analyze the Thickness of the Hippocampus From 7 T MRI. IEEE Transactions on Biomedical Engineering, 2021, 68, 393-403.	2.5	0
8	A selfâ€decoupled 32â€channel receive array for humanâ€brain MRI at 10.5 T. Magnetic Resonance in Medicine, 2021, 86, 1759-1772.	1.9	11
9	Three-dimensional vortex characterization in small intracranial aneurysms based on four dimensional flow magnetic resonance imaging at 7 Tesla. AIP Advances, 2021, 11, .	0.6	1
10	7T Epilepsy Task Force Consensus Recommendations on the Use of 7T MRI in Clinical Practice. Neurology, 2021, 96, 327-341.	1.5	52
11	In vivo human head MRI at 10.5T: A radiofrequency safety study and preliminary imaging results. Magnetic Resonance in Medicine, 2020, 84, 484-496.	1.9	59
12	First inâ€vivo human imaging at 10.5T: Imaging the body at 447 MHz. Magnetic Resonance in Medicine, 2020, 84, 289-303.	1.9	53
13	10.5ÂT MRI static field effects on human cognitive, vestibular, and physiological function. Magnetic Resonance Imaging, 2020, 73, 163-176.	1.0	23
14	Introduction of the snake antenna array: Geometry optimization of a sinusoidal dipole antenna for 10.5T body imaging with lower peak SAR. Magnetic Resonance in Medicine, 2020, 84, 2885-2896.	1.9	25
15	Bilateral Multiband 4D Flow MRI of the Carotid Arteries at 7T. Magnetic Resonance in Medicine, 2020, 84, 1947-1960.	1.9	7
16	Improving radiofrequency power and specific absorption rate management with bumped transmit elements in ultraâ€nigh field MRI. Magnetic Resonance in Medicine, 2020, 84, 3485-3493.	1.9	19
17	A field-monitoring-based approach for correcting eddy-current-induced artifacts of up to the 2nd spatial order in human-connectome-project-style multiband diffusion MRI experiment at 7T: A pilot study. NeuroImage, 2020, 216, 116861.	2.1	13
18	CONtrast Conformed Electrical Properties Tomography (CONCEPT) Based on Multi- Channel Transmission and Alternating Direction Method of Multipliers. IEEE Transactions on Medical Imaging, 2019, 38, 349-359.	5.4	10

#	Article	IF	CITATIONS
19	Automated gradient-based electrical properties tomography in the human brain using 7†Tesla MRI. Magnetic Resonance Imaging, 2019, 63, 258-266.	1.0	7
20	Eliminating susceptibility induced hyperintensities in T1w MPRAGE brain images at 7â€T. Magnetic Resonance Imaging, 2019, 63, 274-279.	1.0	2
21	A Coaxial RF Applicator for Ultra-High Field Human MRI. IEEE Transactions on Biomedical Engineering, 2019, 66, 2848-2854.	2.5	1
22	Brain imaging with improved acceleration and SNR at 7 Tesla obtained with 64â€channel receive array. Magnetic Resonance in Medicine, 2019, 82, 495-509.	1.9	53
23	Excitation and RF Field Control of a Human-Size 10.5-T MRI System. IEEE Transactions on Microwave Theory and Techniques, 2019, 67, 1184-1196.	2.9	5
24	Human Connectome Project-style resting-state functional MRI at 7 Tesla using radiofrequency parallel transmission. Neurolmage, 2019, 184, 396-408.	2.1	22
25	Mapping electrical properties heterogeneity of tumor using boundary informed electrical properties tomography (BIEPT) at 7T. Magnetic Resonance in Medicine, 2019, 81, 393-409.	1.9	13
26	Highâ€resolution wholeâ€brain diffusion MRI at 7T using radiofrequency parallel transmission. Magnetic Resonance in Medicine, 2018, 80, 1857-1870.	1.9	31
27	Quantitative single breathâ€hold renal arterial spin labeling imaging at 7T. Magnetic Resonance in Medicine, 2018, 79, 815-825.	1.9	12
28	Hemodynamics in a giant intracranial aneurysm characterized by in vitro 4D flow MRI. PLoS ONE, 2018, 13, e0188323.	1.1	37
29	Simultaneous multislice imaging in dynamic cardiac MRI at 7T using parallel transmission. Magnetic Resonance in Medicine, 2017, 77, 1010-1020.	1.9	37
30	In vivo imaging of electrical properties of an animal tumor model with an 8â€channel transceiver array at 7 T using electrical properties tomography. Magnetic Resonance in Medicine, 2017, 78, 2157-2169.	1.9	22
31	Patch-Probe Excitation for Ultrahigh Magnetic Field Wide-Bore MRI. IEEE Transactions on Microwave Theory and Techniques, 2017, 65, 2547-2557.	2.9	6
32	Toward imaging the body at 10.5 tesla. Magnetic Resonance in Medicine, 2017, 77, 434-443.	1.9	79
33	Motion-robust cardiac B1+ mapping at 3T using interleaved bloch-siegert shifts. Magnetic Resonance in Medicine, 2017, 78, 670-677.	1.9	11
34	A 16-channel transceiver loop+dipole antennas head array for human head imaging at 10.5T. , 2017, , .		5
35	Optimization and simulation of a 16-channel loop and dipole array for head MRI applications at 10.5 Tesla. , 2017, , .		6
36	Direct imaging of radio-frequency modes via traveling wave magnetic resonance imaging. Journal of Applied Physics, 2016, 119, .	1.1	3

#	Article	IF	CITATIONS
37	Towards highâ€resolution 4D flow MRI in the human aorta using ktâ€GRAPPA and B1+ shimming at 7T. Journal of Magnetic Resonance Imaging, 2016, 44, 486-499.	1.9	25
38	A generalized slabâ€wise framework for parallel transmit multiband RF pulse design. Magnetic Resonance in Medicine, 2016, 75, 1444-1456.	1.9	22
39	Distributing coil elements in three dimensions enhances parallel transmission multiband <scp>RF</scp> performance: A simulation study in the human brain at 7 Tesla. Magnetic Resonance in Medicine, 2016, 75, 2464-2472.	1.9	21
40	Intra-subject multi-slab registration: Application to hippocampal ultra-high resolution imaging at 7T. , 2016, , .		0
41	Simultaneous Quantitative Imaging of Electrical Properties and Proton Density From \$B_{1}\$ Maps Using MRI. IEEE Transactions on Medical Imaging, 2016, 35, 2064-2073.	5.4	12
42	Robust imaging of hippocampal inner structure at 7T: in vivo acquisition protocol and methodological choices. Magnetic Resonance Materials in Physics, Biology, and Medicine, 2016, 29, 475-489.	1.1	7
43	Development and evaluation of a multichannel endorectal RF coil for prostate MRI at 7T in combination with an external surface array. Journal of Magnetic Resonance Imaging, 2016, 43, 1279-1287.	1.9	19
44	Direct control of the temperature rise in parallel transmission by means of temperature virtual observation points: Simulations at 10.5 tesla. Magnetic Resonance in Medicine, 2016, 75, 249-256.	1.9	26
45	Travelling-wave excitation for 16.4T small-bore MRI. , 2015, , .		6
46	Gradientâ€based electrical properties tomography (g <scp>EPT</scp>): A robust method for mapping electrical properties of biological tissues in vivo using magnetic resonance imaging. Magnetic Resonance in Medicine, 2015, 74, 634-646.	1.9	80
47	Design of parallel transmission radiofrequency pulses robust against respiration in cardiac MRI at 7 Tesla. Magnetic Resonance in Medicine, 2015, 74, 1291-1305.	1.9	34
48	Comparison of RF body coils for MRI at 3  T: a simulation study using parallel transmission on various anatomical targets. NMR in Biomedicine, 2015, 28, 1332-1344.	1.6	28
49	High-Resolution Mapping of Myeloarchitecture In Vivo: Localization of Auditory Areas in the Human Brain. Cerebral Cortex, 2015, 25, 3394-3405.	1.6	90
50	Presurgical Functional Localization Possibilities, Limitations, and Validity. Medical Radiology, 2015, , 247-267.	0.0	1
51	Quantitative prediction of radio frequency induced local heating derived from measured magnetic field maps in magnetic resonance imaging: A phantom validation at 7 T. Applied Physics Letters, 2014, 105, 244101.	1.5	19
52	Gradient-based magnetic resonance electrical properties imaging of brain tissues. , 2014, 2014, 6056-9.		0
53	Predicting temperature increase through local SAR estimation by B1 mapping: A phantom validation at 7T. , 2014, 2014, 1107-10.		1
54	Seven-Tesla Time-of-Flight Angiography Using a 16-Channel Parallel Transmit System With Power-Constrained 3-dimensional Spoke Radiofrequency Pulse Design. Investigative Radiology, 2014, 49, 314-325.	3.5	29

#	Article	IF	CITATIONS
55	Cerebral TOF angiography at 7T: Impact of <i>B</i> ₁ ⁺ shimming with a 16â€channel transceiver array. Magnetic Resonance in Medicine, 2014, 71, 966-977.	1.9	32
56	Mitigating transmit B 1 inhomogeneity in the liver at 7T using multi-spoke parallel transmit RF pulse design. Quantitative Imaging in Medicine and Surgery, 2014, 4, 4-10.	1.1	38
57	Dynamically applied <i>B</i> ₁ ⁺ shimming solutions for nonâ€contrast enhanced renal angiography at 7.0 tesla. Magnetic Resonance in Medicine, 2013, 69, 114-126.	1.9	57
58	Complex B ₁ mapping and electrical properties imaging of the human brain using a 16â€channel transceiver coil at 7T. Magnetic Resonance in Medicine, 2013, 69, 1285-1296.	1.9	65
59	Intracranial-Derived Atherosclerosis Assessment: An In Vitro Comparison between Virtual Histology by Intravascular Ultrasonography, 7T MRI, and Histopathologic Findings. American Journal of Neuroradiology, 2013, 34, 2259-2264.	1.2	54
60	From Complex <formula formulatype="inline"><tex notation="TeX">\${m B}_{1}\$</tex></formula> Mapping to Local SAR Estimation for Human Brain MR Imaging Using Multi-Channel Transceiver Coil at 7T. IEEE Transactions on Medical Imaging, 2013, 32, 1058-1067.	5.4	60
61	Pushing spatial and temporal resolution for functional and diffusion MRI in the Human Connectome Project. NeuroImage, 2013, 80, 80-104.	2.1	769
62	Simultaneous multislice multiband parallel radiofrequency excitation with independent slice-specific transmit B1 homogenization. Magnetic Resonance in Medicine, 2013, 70, 630-638.	1.9	63
63	Determining electrical properties based on <i>B</i> ₁ fields measured in an MR scanner using a multi-channel transmit/receive coil: a general approach. Physics in Medicine and Biology, 2013, 58, 4395-4408.	1.6	44
64	Spatial organization of frequency preference and selectivity in the human inferior colliculus. Nature Communications, 2013, 4, 1386.	5.8	89
65	Cardiac imaging at 7 tesla: Single―and twoâ€spoke radiofrequency pulse design with 16â€channel parallel excitation. Magnetic Resonance in Medicine, 2013, 70, 1210-1219.	1.9	58
66	Inversion recovery at 7 T in the human myocardium: Measurement of <i>T</i> ₁ , inversion efficiency and <i>B</i> ₁ ⁺ . Magnetic Resonance in Medicine, 2013, 70, 1038-1046.	1.9	39
67	Correcting for Strong Eddy Current Induced B0 Modulation Enables Two-Spoke RF Pulse Design with Parallel Transmission: Demonstration at 9.4T in the Human Brain. PLoS ONE, 2013, 8, e78078.	1.1	17
68	Spin echo functional MRI in bilateral auditory cortices at 7T: An application of B1 shimming. Neurolmage, 2012, 63, 1313-1320.	2.1	22
69	Comparison between eight―and sixteenâ€channel TEM transceive arrays for body imaging at 7 T. Magnetic Resonance in Medicine, 2012, 67, 954-964.	1.9	54
70	Contrast enhancement in TOF cerebral angiography at 7 T using saturation and MT pulses under SAR constraints: Impact of VERSE and sparse pulses. Magnetic Resonance in Medicine, 2012, 68, 188-197.	1.9	35
71	7 Tesla (T) human cardiovascular magnetic resonance imaging using FLASH and SSFP to assess cardiac function: validation against 1.5 T and 3 T NMR in Biomedicine, 2012, 25, 27-34.	1.6	57
72	Regional neurochemical profiles in the human brain measured by ¹ H MRS at 7 T using local <i>B</i> ₁ shimming. NMR in Biomedicine, 2012, 25, 152-160.	1.6	104

#	Article	IF	CITATIONS
73	Localized ¹ H NMR spectroscopy in different regions of human brain <i>in vivo</i> at 7 T: <i>T</i> ₂ relaxation times and concentrations of cerebral metabolites. NMR in Biomedicine, 2012, 25, 332-339.	1.6	117
74	Simultaneous bilateral hip joint imaging at 7 Tesla using fast transmit B ₁ shimming methods and multichannel transmission – a feasibility study. NMR in Biomedicine, 2012, 25, 1202-1208.	1.6	33
75	Whole brain high-resolution functional imaging at ultra high magnetic fields: An application to the analysis of resting state networks. NeuroImage, 2011, 57, 1031-1044.	2.1	68
76	Mapping the Organization of Axis of Motion Selective Features in Human Area MT Using High-Field fMRI. PLoS ONE, 2011, 6, e28716.	1.1	163
77	Hippocampal Sclerosis in Temporal Lobe Epilepsy: Findings at 7 T. Radiology, 2011, 261, 199-209.	3.6	104
78	084â€High field (7 Tesla) cardiovascular MRI: a feasibility and comparison study. Heart, 2010, 96, A51-A52.	1.2	1
79	Retinotopic mapping with spin echo BOLD at 7T. Magnetic Resonance Imaging, 2010, 28, 1258-1269.	1.0	45
80	Parallel excitation in the human brain at 9.4 T counteracting <i>k</i> â€space errors with RF pulse design. Magnetic Resonance in Medicine, 2010, 63, 524-529.	1.9	43
81	A 32â€channel lattice transmission line array for parallel transmit and receive MRI at 7 tesla. Magnetic Resonance in Medicine, 2010, 63, 1478-1485.	1.9	80
82	Performance of external and internal coil configurations for prostate investigations at 7 T. Magnetic Resonance in Medicine, 2010, 64, 1625-1639.	1.9	63
83	Adapted RF pulse design for SAR reduction in parallel excitation with experimental verification at 9.4T. Journal of Magnetic Resonance, 2010, 205, 161-170.	1.2	25
84	In vivo 1H NMR spectroscopy of the human brain at 9.4T: Initial results. Journal of Magnetic Resonance, 2010, 206, 74-80.	1.2	99
85	Dynamics of motor-related functional integration during motor sequence learning. Neurolmage, 2010, 49, 759-766.	2.1	117
86	MP2RAGE, a self bias-field corrected sequence for improved segmentation and T1-mapping at high field. NeuroImage, 2010, 49, 1271-1281.	2.1	1,075
87	Adapted RF pulse design for SAR reduction in parallel excitation with experimental verification at 9.4 T. Journal of Magnetic Resonance, 2010, 205, 161-70.	1.2	11
88	Initial results of cardiac imaging at 7 tesla. Magnetic Resonance in Medicine, 2009, 61, 517-524.	1.9	143
89	Exploring the promise land of 7 T for CMR with T-PAT accelerated imaging techniques – first results for real time cardiac function and tagging in volunteers. Journal of Cardiovascular Magnetic Resonance, 2009, 11, .	1.6	0
90	T1 weighted brain images at 7ÂTesla unbiased for Proton Density, T2⎠contrast and RF coil receive B1 sensitivity with simultaneous vessel visualization. NeuroImage, 2009, 46, 432-446.	2.1	260

#	Article	IF	CITATIONS
91	Ultra-high field parallel imaging of the superior parietal lobule during mental maze solving. Experimental Brain Research, 2008, 187, 551-561.	0.7	19
92	Local <i>B</i> ₁ ⁺ shimming for prostate imaging with transceiver arrays at 7T based on subjectâ€dependent transmit phase measurements. Magnetic Resonance in Medicine, 2008, 59, 396-409.	1.9	289
93	A geometrically adjustable 16â€channel transmit/receive transmission line array for improved RF efficiency and parallel imaging performance at 7 Tesla. Magnetic Resonance in Medicine, 2008, 59, 590-597.	1.9	181
94	Human brain glycogen content and metabolism: implications on its role in brain energy metabolism. American Journal of Physiology - Endocrinology and Metabolism, 2007, 292, E946-E951.	1.8	114
95	Enhanced relative BOLD signal changes in <i>T</i> ₂ â€weighted stimulated echoes. Magnetic Resonance in Medicine, 2007, 58, 754-762.	1.9	15
96	Dynamics of lactate concentration and blood oxygen level-dependent effect in the human visual cortex during repeated identical stimuli. Journal of Neuroscience Research, 2007, 85, 3340-6.	1.3	58
97	Sustained Neuronal Activation Raises Oxidative Metabolism to a New Steady-State Level: Evidence from 1H NMR Spectroscopy in the Human Visual Cortex. Journal of Cerebral Blood Flow and Metabolism, 2007, 27, 1055-1063.	2.4	253
98	Validity of Presurgical Functional Localization. Medical Radiology, 2007, , 167-187.	0.0	7
99	Reducing temporal fluctuations in MRI with the multichannel method SENSE. , 2006, , .		0
100	Sensitivity of single-voxel 1H-MRS in investigating the metabolism of the activated human visual cortex at 7 T. Magnetic Resonance Imaging, 2006, 24, 343-348.	1.0	115
101	Potential and feasibility of parallel MRI at high field. NMR in Biomedicine, 2006, 19, 368-378.	1.6	113
102	Application of parallel imaging to fMRI at 7 Tesla utilizing a high 1D reduction factor. Magnetic Resonance in Medicine, 2006, 56, 118-129.	1.9	32
103	9.4T human MRI: Preliminary results. Magnetic Resonance in Medicine, 2006, 56, 1274-1282.	1.9	278
104	Motor control in basal ganglia circuits using fMRI and brain atlas approaches. Cerebral Cortex, 2006, 16, 149-161.	1.6	227
105	High Magnetic Fields for Imaging Cerebral Morphology, Function, and Biochemistry. Biological Magnetic Resonance, 2006, , 285-342.	0.4	8
106	Transmit and receive transmission line arrays for 7 Tesla parallel imaging. Magnetic Resonance in Medicine, 2005, 53, 434-445.	1.9	374
107	B1 destructive interferences and spatial phase patterns at 7 T with a head transceiver array coil. Magnetic Resonance in Medicine, 2005, 54, 1503-1518.	1.9	416
108	Distinct basal ganglia territories are engaged in early and advanced motor sequence learning. Proceedings of the National Academy of Sciences of the United States of America, 2005, 102, 12566-12571.	3.3	521

#	Article	IF	CITATIONS
109	Signal and noise characteristics of Hahn SE and GE BOLD fMRI at 7 T in humans. NeuroImage, 2005, 24, 738-750.	2.1	182
110	3-D Diffusion Tensor Axonal Tracking shows Distinct SMA and Pre-SMA Projections to the Human Striatum. Cerebral Cortex, 2004, 14, 1302-1309.	1.6	260
111	Diffusion tensor fiber tracking shows distinct corticostriatal circuits in humans. Annals of Neurology, 2004, 55, 522-529.	2.8	498
112	Parallel imaging performance as a function of field strength?An experimental investigation using electrodynamic scaling. Magnetic Resonance in Medicine, 2004, 52, 953-964.	1.9	179
113	Distinct striatal regions support movement selection, preparation and execution. NeuroReport, 2004, 15, 2327-2331.	0.6	82
114	Motor execution and imagination networks in post-stroke dystonia. NeuroReport, 2004, 15, 1887-1890.	0.6	42
115	Ultrahigh field magnetic resonance imaging and spectroscopy. Magnetic Resonance Imaging, 2003, 21, 1263-1281.	1.0	218
116	Spin-echo fMRI in humans using high spatial resolutions and high magnetic fields. Magnetic Resonance in Medicine, 2003, 49, 655-664.	1.9	284
117	Spatial dependence of the nonlinear BOLD response at short stimulus duration. NeuroImage, 2003, 18, 990-1000.	2.1	73
118	Mirror-Symmetric Tonotopic Maps in Human Primary Auditory Cortex. Neuron, 2003, 40, 859-869.	3.8	421
119	Bilateral hemispheric alteration of memory processes in right medial temporal lobe epilepsy. Journal of Neurology, Neurosurgery and Psychiatry, 2002, 73, 478-485.	0.9	57
120	Late plasticity for language in a child's nonâ€dominant hemisphere. Brain, 2002, 125, 361-372.	3.7	286
121	Effect of Impaired Recognition and Expression of Emotions on Frontocingulate Cortices: An fMRI Study of Men With Alexithymia. American Journal of Psychiatry, 2002, 159, 961-967.	4.0	247
122	Zoomed Functional Imaging in the Human Brain at 7 Tesla with Simultaneous High Spatial and High Temporal Resolution. NeuroImage, 2002, 17, 272-286.	2.1	134
123	Sustained Negative BOLD, Blood Flow and Oxygen Consumption Response and Its Coupling to the Positive Response in the Human Brain. Neuron, 2002, 36, 1195-1210.	3.8	565
124	Correction of physiologically induced global off-resonance effects in dynamic echo-planar and spiral functional imaging. Magnetic Resonance in Medicine, 2002, 47, 344-353.	1.9	212
125	Respiration-inducedB0 fluctuations and their spatial distribution in the human brain at 7 Tesla. Magnetic Resonance in Medicine, 2002, 47, 888-895.	1.9	225
126	Perfusion-based high-resolution functional imaging in the human brain at 7 Tesla. Magnetic Resonance in Medicine, 2002, 47, 903-911.	1.9	117

#	Article	IF	CITATIONS
127	Magnetic resonance imaging of brain function and neurochemistry. Proceedings of the IEEE, 2001, 89, 1093-1106.	16.4	4
128	Delayed Verbal Memory Retrieval: A Functional MRI Study in Epileptic Patients with Structural Lesions of the Left Medial Temporal Lobe. NeuroImage, 2001, 14, 995-1003.	2.1	57
129	Functional imaging in the work-up of childhood epilepsy. Child's Nervous System, 2001, 17, 223-228.	0.6	32
130	Elimination of k-space spikes in fMRI data. Magnetic Resonance Imaging, 2001, 19, 1037-1041.	1.0	18
131	Slice acquisition order and blood oxygenation level dependent frequency content: an event-related functional magnetic resonance imaging study. Magnetic Resonance Materials in Physics, Biology, and Medicine, 2001, 13, 91-100.	1.1	2
132	Imaging brain function in humans at 7 Tesla. Magnetic Resonance in Medicine, 2001, 45, 588-594.	1.9	421
133	Artifact due toB0 fluctuations in fMRI: Correction using thek-space central line. Magnetic Resonance in Medicine, 2001, 46, 198-201.	1.9	51
134	Investigation of the initial dip in fMRI at 7 Tesla. NMR in Biomedicine, 2001, 14, 408-412.	1.6	108
135	Interaction of Gustatory and Lingual Somatosensory Perceptions at the Cortical Level in the Human: a Functional Magnetic Resonance Imaging Study. Chemical Senses, 2001, 26, 371-383.	1.1	185
136	Understanding dissociations in dyscalculia. Brain, 2000, 123, 2240-2255.	3.7	348
137	Visual Perception of Motion and 3-D Structure from Motion: an fMRI Study. Cerebral Cortex, 2000, 10, 772-783.	1.6	122
138	Episodic memory in left temporal lobe epilepsy: a functional MRI study. Brain, 2000, 123, 1722-1732.	3.7	145
139	Distinct Cortical Areas for Names of Numbers and Body Parts Independent of Language and Input Modality. NeuroImage, 2000, 12, 381-391.	2.1	131
140	365. Emotion-inducing stimuli processing in alexithymia: an fMRI study. Biological Psychiatry, 2000, 47, S110.	0.7	5
141	Differential Contributions of the Left and Right Inferior Parietal Lobules to Number Processing. Journal of Cognitive Neuroscience, 1999, 11, 617-630.	1.1	513
142	Cortical Areas Activated by Bilateral Galvanic Vestibular Stimulation. Annals of the New York Academy of Sciences, 1999, 871, 313-323.	1.8	49
143	Distinct prefrontal activations in processing sequence at the sentence and script level: An fMRI study. Neuropsychologia, 1999, 37, 1469-1476.	0.7	120
144	Field-frequency locked in vivo proton MRS on a whole-body spectrometer. Magnetic Resonance in Medicine, 1999, 42, 636-642.	1.9	67

#	Article	IF	CITATIONS
145	Human taste cortical areas studied with functional magnetic resonance imaging: evidence of functional lateralization related to handedness. Neuroscience Letters, 1999, 277, 189-192.	1.0	118
146	An Anatomical Landmark for the Supplementary Eye Fields in Human Revealed with Functional Magnetic Resonance Imaging. Cerebral Cortex, 1999, 9, 705-711.	1.6	162
147	Event-related fMRI analysis of the cerebral circuit for number comparison. NeuroReport, 1999, 10, 1473-1479.	0.6	180
148	Imaging unconscious semantic priming. Nature, 1998, 395, 597-600.	13.7	1,100
149	Inferring behavior from functional brain images. Nature Neuroscience, 1998, 1, 549-549.	7.1	33
150	Functional Lateralization of Human Gustatory Cortex Related to Handedness Disclosed by fMRI Studya. Annals of the New York Academy of Sciences, 1998, 855, 575-578.	1.8	58
151	Somatotopical organization of striatal activation during finger and toe movement: A 3-T functional magnetic resonance imaging study. Annals of Neurology, 1998, 44, 398-404.	2.8	59
152	Anatomical variability in the cortical representation of first and second language. NeuroReport, 1997, 8, 3809-3815.	0.6	524
153	Latencies in fMRI time-series: effect of slice acquisition order and perception. , 1997, 10, 230-236.		43
154	Regulation of T helper-B lymphocyte adhesion through CD4-HLA class II interaction. European Journal of Immunology, 1990, 20, 637-644.	1.6	40
155	Seizure disorders. , 0, , 519-525.		0
156	CHAPTER 24. Ultrahigh-Field Whole-Body MRI for Cartilage Imaging: Technical Challenges. New Developments in NMR, 0, , 671-705.	0.1	0